Nanostructured Au–CeO_2 catalysts for low-temperature water–gas shift

Qi Fu, Adam Weber * and Maria Flytzani-Stephanopoulos **

Department of Chemical and Biological Engineering, Tufts University, 4 Colby Street, Medford, MA 02155, USA
E-mail: maria.flytzani-stephanopoulos@tufts.edu

Received 6 April 2001; accepted 6 July 2001

The composite system of nanostructured gold and cerium oxide, with a gold loading 5–8 wt%, is reported in this work as a very good catalyst for low-temperature water–gas shift. Activity depends largely on the presence of nanosized ceria particles. Various techniques of preparation of an active catalyst are disscussed. The presence of gold is crucial for activity below 300 °C. A dramatic effect of gold on the reducibility of the surface oxygen of ceria is found by H_2-TPR, from 310–480 °C to 25–110 °C. All of the available surface oxygen was reduced, while there was no effect on the bulk oxygen of ceria. This correlates well with the shift activity of the Au–ceria system.

KEY WORDS: cerium oxide; gold nanoparticles; water–gas shift catalysts; temperature-programmed reduction; redox reaction mechanism

1. Introduction

There is presently a renewed interest in the water–gas shift reaction for application to fuel processing for fuel cell-power generation. Advanced low-temperature shift (LTS) catalysts are needed to produce essentially CO-free hydrogen to feed the PEM fuel cells under development for automobiles. Desired catalyst characteristics include high activity and stability over a wider operating temperature window than is currently possible with the commercial LTS catalysts.

Catalysts based on cerium oxide are promising for these applications [1,2]. Ceria is widely used as an oxygen storage component in the automobile three-way catalyst, releasing/accepting oxygen under fuel-rich/lean conditions in the exhaust gas stream. Additionally, ceria is a better choice than alumina as a support for the noble metals in the catalytic converter because it drastically improves their low-temperature activity for CO oxidation [3] and the water–gas shift reaction [2]. In recent work, we have shown that similarly active are combinations of ceria with a variety of base metals and metal oxides [1,4–7]. The enhanced activity of these catalysts has been attributed to a synergistic redox reaction mechanism. Metal-modified cerium oxide has a higher oxygen storage capacity (OSC) and reducibility than pure ceria [1,2,4,8,9]. We have recently reported that Cu–ceria is much more stable than Cu–ZnO-based LTS catalysts, retaining high WGS activity and structural stability at temperatures as high as 650 °C [1,10,11].

Gold supported on ceria is a very good, albeit much less studied, catalyst system for redox reactions. It has been shown to possess high activity for CO oxidation [4–7,12], and methane oxidation [4–6], and, in recent work in this lab, it was found promising for low-temperature WGS [7,11]. The Au–ceria catalyst [7] is more stable than the well-studied Au–TiO_2 [13–15] system for low-temperature CO oxidation.

Gold on other reducible oxides has been reported to be active for low temperature water–gas shift [16–19]. Andreeva and coworkers [16,18] found good WGS activity in fine metallic gold particles on iron oxide (Au/α-Fe_2O_3) prepared by coprecipitation. Sakurai *et al.* [17] reported that Au/TiO_2, prepared by deposition–precipitation, has comparable LTS activity to that of commercial Cu/ZnO/Al_2O_3 catalysts. More recently, Au supported on ZnO and ZrO_2 has also been found active for the water–gas shift reaction [19].

It is interesting to evaluate these systems from the point of view of the gold particle structure as well as the structure of the reducible oxide. The importance of nanosized Au particles for a variety of reactions has been recognized and ample attention has been paid to their study over the past decade. Yet, much less attention has been given to the properties of the reducible oxide support [15,19,20], even though this is considered crucial as a source of oxygen [15,20] or for otherwise stabilizing Au in the active nanostructured form [15,21]. The Au particle size and structure are sensitive to a number of variables, including the preparation method [15], the state and structure of the support [15,19,20], and catalyst pretreatment [22].

The preparation method has been reported to directly affect the activity of the Au-reducible oxide system. The currently employed methods of coprecipitation [13], deposition–precipitation [23], impregnation [22], co-sputtering [24], and chemical vapor deposition [25] can achieve highly dispersed gold particles with diameters below 5 nm. However, a different preparation method is preferred for

* Present address: Department of Chemical Engineering, University of California, Berkeley, USA.
** To whom correspondence should be addressed.

1011-372X/01/1100-0087$19.50/0

each reducible oxide support. Recently, Kozlov and coworkers [21,26] reported a new synthesis method, which employs Au phosphine complexes and clusters and as-precipitated wet metal hydroxides as precursors. The simultaneous decomposition of Au complexes and phase change of support achieves more efficient Au–support interaction, and therefore, more active and stable Au catalysts. Other methods are under evaluation, for instance, the method of using gold colloids whose particle size is established before deposition on the supports [27] to get better gold size control.

In this paper, two commonly used preparation methods, namely: coprecipitation and deposition–precipitation, were used to prepare gold on cerium oxide. Additionally, the urea gelation/precipitation method [1,28] was used to prepare one of the Au–ceria samples reported here. Characterization of both the ceria and gold particles is reported. The WGS reaction rate over these Au–ceria samples was measured at 100 and 175 °C, and correlated to the catalyst structural properties.

2. Experimental

2.1. Catalyst preparation

In the work on Au/ceria reported by Liu *et al.* [4–6], a conventional coprecipitation method using ammonium carbonate as the precipitant was used to prepare the catalyst. In more recent work, Weber [7] studied various preparation methods and conducted a full parametric study of each method in his effort to optimize the activity of this type of catalyst for CO oxidation. From that work, a deposition–precipitation technique was found the most promising.

Based on the above findings [4–7], two preparation methods were examined in this work. Coprecipitation (CP) involves mixing aqueous solutions of $HAuCl_4$, cerium(III) nitrate and lanthanum nitrate with $(NH_4)CO_3$ at 60–70 °C, keeping a constant pH value of 8 and aging the resulting precipitate at 60–70 °C for 1 h. After aging, the precipitate was filtered and washed with distilled water until there were no residual Cl^- ions as tested by $AgNO_3$ solution. Further, the precipitate was dried at 100–120 °C, then heated to 400 °C in air at a heating rate of 2 °C/min; calcination at 400 °C continued for 10 h.

Alternatively, deposition–precipitation (DP) was used [7,11]. Unlike coprecipitation, the catalyst support was already prepared and calcined prior to its use in the DP method. The doped and undoped ceria was prepared by the urea gelation/coprecipitation (UGC) method described in [1]. The cerium salt used was $(NH_4)_2Ce(NO_3)_6$. In brief, urea (H_2N–CO–NH_2) was added into the aqueous nitrate solutions and heated to 100 °C under vigorous stirring and addition of deionized water. The resulting gel was kept for 8 h at 100 °C; the subsequent filtering, and heating steps were as described above. Some samples were calcined at 650 °C for 4 h. Deposition–precipitation took place by adding the desired amount of $HAuCl_4$ dropwise into an aqueous slurry of the thus prepared ceria. The pH of the aqueous slurry had already been adjusted to the value of 8 using $(NH_4)_2CO_3$. The resulting precipitate was aged at room temperature for 1 h, then filtered, washed and heat treated as above. Unlike the deposition–precipitation method reported by Tsubota *et al.* [23] which uses NaOH base and excess (about five times) $HAuCl_4$, the present method can deposit the desired gold loading on ceria using the exact amount of $HAuCl_4$ solution [7]. One sample containing a large loading (8 at%) of gold in ceria was prepared by the above urea gelation/coprecipitation technique (UGC), but at lower temperature (80 °C).

All reagents used in catalyst preparation were analytical grade. The samples reported here are denoted as αAu-CL (z, T), where α is the atomic % gold loading [$100 \times (\mathrm{Au}/\mathrm{M_{Au}})/(\mathrm{Au}/\mathrm{M_{Au}} + \mathrm{Ce}/\mathrm{M_{Ce}} + \mathrm{La}/\mathrm{M_{La}})$], z is the method of preparation: CP, DP, or UGC, and T is the calcination temperature. This will be noted only if it differs from 400 °C, the typical catalyst calcination temperature used for most samples. The lanthanum doping of ceria is around 10 at%. These samples are denoted as CL. A few samples were prepared with 4 at% lanthanum in ceria for comparison. These are denoted as C4L.

2.2. Catalyst characterization and activity tests

The bulk elemental composition of each sample was determined by inductively coupled plasma (ICP) atomic emission spectrometry (Perkin–Elmer, Plasma 40). The total sample surface area was measured by single-point BET N_2 adsorption/desorption on a Micromeritics Pulse ChemiSorb 2705.

X-ray powder diffraction (XRD) analysis of the samples was performed on a Rigaku 300 X-ray diffractometer with rotating anode generators and a monochromatic detector. Copper Kα radiation was used. The crystal size of ceria and gold was calculated from the peak broadening using the Scherrer equation [29].

The catalyst morphology and elemental distribution analysis was performed with a Vacuum Generators HB603 scanning transmission electron microscope (STEM) equipped with a X-ray microprobe of 0.14 nm optimum resolution for energy dispersive X-ray spectroscopy (EDS). For STEM analysis, the catalyst powder was dispersed on a copper or nickel grid coated with a carbon film and elemental maps were obtained on a 128 × 128 data matrix.

WGS reaction tests and kinetics measurements were conducted with the catalyst in powder form (<150 μm) in the microreactor assemblies described in a previous paper [1]. All samples were used in the prepared form without activation. The total gas flow rate used in the reaction tests was 100 cm^3/min (NTP), and the space time was 0.09 g s/cm^3. In the kinetic tests, the conversion of CO was kept <15% by adjusting either the amount of the catalyst or the total gas flow rate. Both the consumption of CO and the production of CO_2 were in balance and either could be used to calculate

the reaction rate. The feed and product gas streams were analyzed by a HP-6890 gas chromatograph equipped with a thermal conductivity detector (TCD). A Carbosphere (Alltech) packed column (6 ft × 1/8 inch) was used to separate CO and CO_2.

Temperature-programmed reduction (TPR) of the as-prepared catalysts in fine powder form (<150 μm) was carried out in the Micromeritics Pulse ChemiSorb 2705 instrument. The samples were first oxidized in a 10% O_2/He gas mixture (50 cm^3/min (STP)) at 350 °C for 30 min. After cooling down to 200 °C in the O_2/He mixture, pure nitrogen (grade 5) was switched in and cooling continued down to room temperature (RT). Then the sample holder was immersed in liquid nitrogen. A 20% H_2/N_2 gas mixture (50 cm^3/min (STP)) was next introduced over the sample causing a hight desorption peak, at the end point of which the liquid N_2 was removed and the sample temperature was raised to RT. A second big desorption peak was recorded at that time. Those two peaks appeared with all samples, even for pure ceria alone, and were identical; thus, they are attributed to desorption of physically adsorbed nitrogen and hydrogen. From RT on, the sample was heated at a rate of 5 °C/min to 900 °C. The change of hydrogen concentration was detected by the TCD of the instrument. A cold trap filled with a mixture of isopropanol and liquid nitrogen was placed in the gas line upstream of the TCD to remove the water vapor.

3. Results and discussion

3.1. Catalyst characterization

Figures 1 and 2 show STEM micrographs and elemental maps, respectively, of CP and DP samples of 5Au-C4L. Figure 1 clearly shows a large difference in the structure of ceria between the CP and DP samples. Although both possess the fluorite oxide structure as evidenced by XRD analysis, see figure 3, the samples prepared by coprecipitation have a needlelike and layered bulk structure while the DP samples have a uniform spherical structure. The 4 at% La-doped ceria used in the DP sample had been prepared by urea gelation/precipitation, and calcined in air at 650 °C. The crystal habit of ceria is thus a function of the type and conditions of precipitation.

Figure 2 shows a uniform distribution of gold on ceria for the DP sample, while the CP sample contains relatively large gold particles with a lower dispersion. This difference of DP over the CP method was also found for gold deposited on several other oxides [14]. Based on the EDS analysis, metallic gold was present in both samples shown in figure 2 [17]. From the STEM analyses as well as independent high resolution TEM [30], we found that the gold particles in the CP sample have an average size of 8 nm, while in the DP sample, gold particles are <5 nm.

The XRD patterns of samples prepared by different methods are shown in figure 3. These comprise CeO_2 and metallic gold crystal phases, which agrees with the STEM/EDS analysis. The distinct fluorite oxide-type diffraction pattern of CeO_2 was observed in all samples. Lanthanum is in oxide solid solution with ceria, so there are no separate reflections from La compounds, in agreement with previous work [1,4–6]. The addition of La inhibits the crystal growth of ceria made by either the CP or the UGC methods [31,32]. The calculated average gold and ceria crystallite size are listed in table 1. With increasing calcination temperature, the particle size of ceria and gold increased and the specific surface area decreased. Since gold was deposited on the UGC pre-calcined ceria in the DP samples, the addition

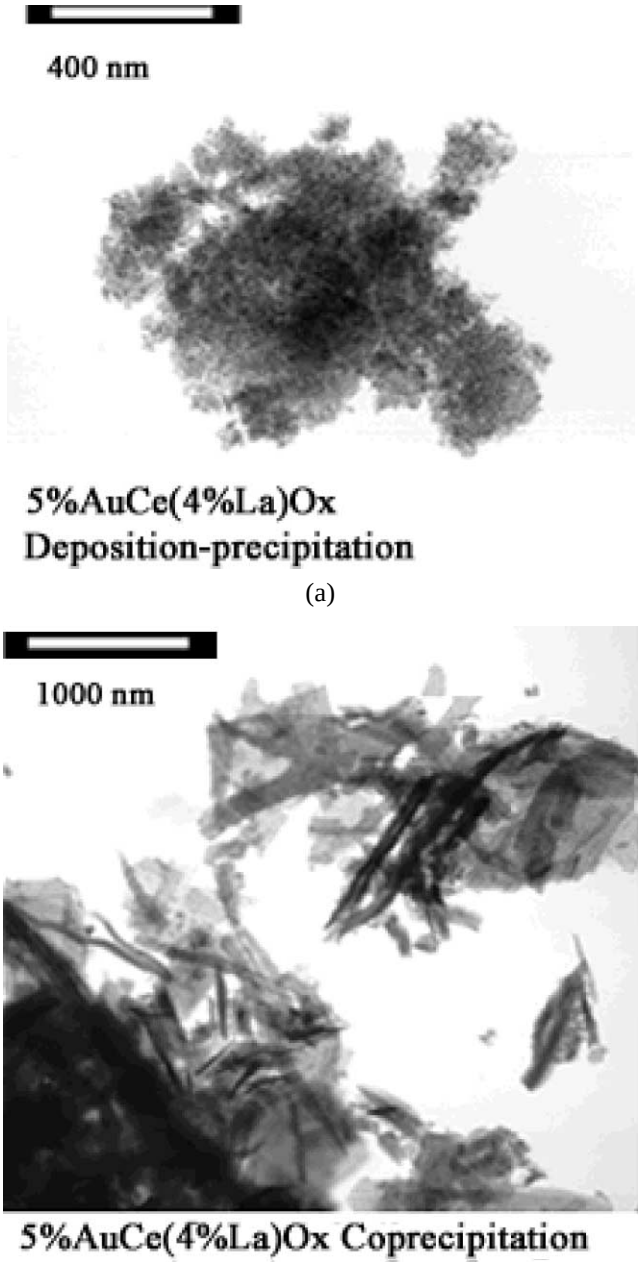

Figure 1. STEM micrographs of Au–ceria samples prepared by (a) deposition–precipitation and (b) coprecipitation. See table 1 for sample identification and preparation conditions.

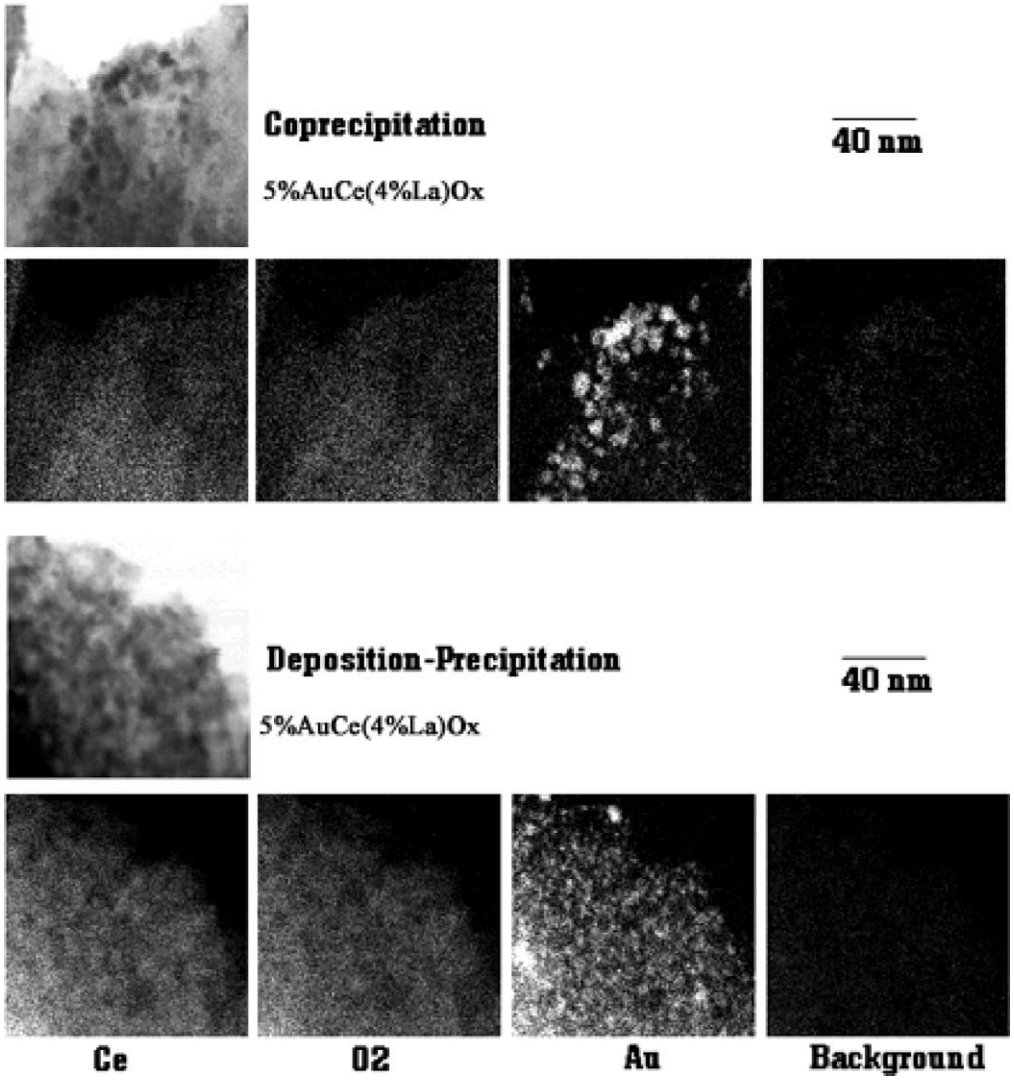

Figure 2. STEM/EDS elemental maps of Au–ceria samples prepared by coprecipitation and deposition–precipitation. See table 1 for sample identification and preparation conditions.

of gold should have no effect on the size and structure of ceria. This is seen in table 1 by comparing the crystallite size of ceria before and after the deposition of gold. However, for the CP samples, the incorporation of gold or copper during coprecipitation may suppress the growth of ceria crystallites during the calcination step [30]. This is seen in table 1 by comparing the particle size of ceria in the Au–ceria and in neat ceria samples prepared by CP. This effect has also been reported for Au/Fe_2O_3 [33–35]. Sze *et al.* proposed that Au can substitute into the Fe_2O_3 unit cell as ions in 3+ state as evidenced by XPS and Mössbauer spectroscopy [33]. As explained by Haruta *et al.* [35], Fe and Au can form an intermetallic bond, since Fe has a slight solubility in gold and the Au–Fe distance is close to but lower than the sum of the metal radii of Au and Fe.

In figure 3, a small broad peak corresponding to Au(111), and a barely visible peak corresponding to Au(200) are seen in the X-ray diffraction patterns of all samples except 0.9Au-CL(DP), which has a very low gold loading. With increasing gold loading, the gold diffraction peak is more pronounced, but the width at half peak maximum (FWHM) remains unchanged. Thus, the gold particle size does not increase with loading. This indicates a strong interaction between gold and ceria.

When the 4.7Au-CL (DP) sample was calcined at 650 °C, see table 1, the gold particle size grew to 9.2 nm, which is much larger than that of the sample calcined at 400 °C (4.6 nm). Thus, there is a significant effect of calcination temperature on the growth of gold particles [23]. Figure 3 also shows the reflections from sample 8Au-CL(UGC), which was prepared by urea gelation/coprecipitation, as described above. The peaks corresponding to Au(111) and Au(200) are big and sharp, with a corresponding average gold particle size of 43 nm, table 1. The ceria particle size, however, was very small (4.5 nm), similar to the size of neat ceria made by the same gelation method at 400 °C. This finding is interesting, because it indicates an independent rate of the growth of the gold and ceria crystals.

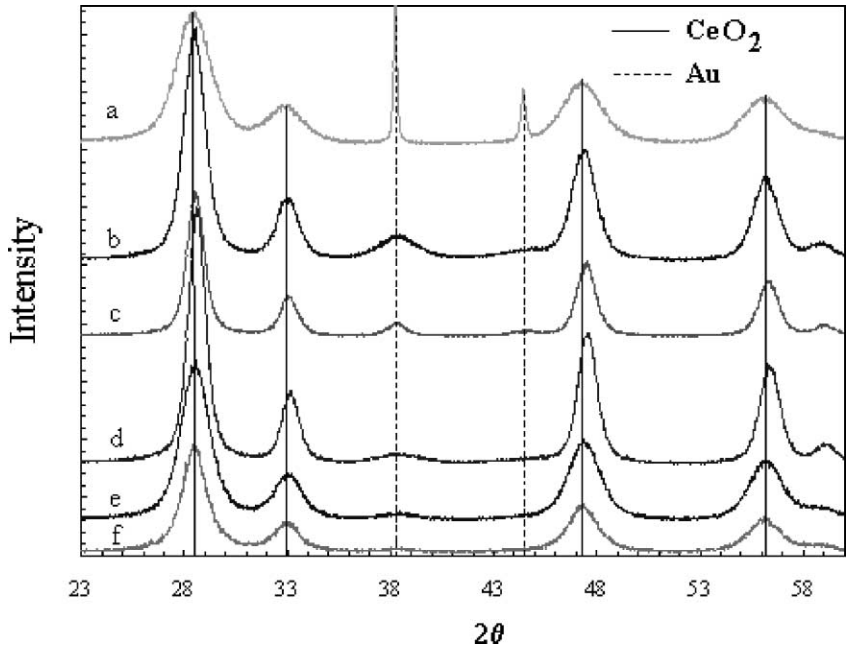

Figure 3. XRD patterns of Au–ceria samples: (a) 8Au-CL(UGC), (b) 8.3Au-CL(DP), (c) 4.7Au-CL(DP)[b,c], (d) 4.7Au-CL(DP)[b], (e) 4.5Au-CL(DP)[a], (f) 3.8Au-CL(CP). See table 1 for sample identification and preparation conditions.

Table 1
Physical properties of ceria-based materials. (All catalysts calcined at 400 °C for 10 h, unless otherwise noted. CL: Ce(10% La)O_x; C4L: Ce(4% La)O_x.)

Sample	BET surface area (m^2/g)	Particle size[e] (nm)		
		Au ⟨111⟩	CeO_2 ⟨111⟩	CeO_2 ⟨220⟩
8.3Au-CL(DP)[b]	93.6	4.5	7.1	6.9
4.7Au-CL(DP)[b,c]	–	9.2	7.1	6.9
4.7Au-CL(DP)[b]	82.7	4.6	7.1	6.9
	71.6[f]	6.8	7.3	7.2
4.5AuC4L(DP)[b]	83	4.6	8.1	8.5
0.9Au-CL(DP)[b]	96.7	–	7.1	6.9
4.5Au-CL(DP)[a]	155.8	5.0	5.2	4.9
	128.4[g]	6.2	5.3	4.9
3.8Au-CL(CP)	71.8	6.7	5.8	5.3
	61.3[f]	7.2	7	6.4
3.9AuC4L(CP)	–	7.9	7.1	7.0
5Cu-CL(UGC)[c,h]	89.1	–	5.2	4.9
5Cu-CL(UGC)[h]	187.1	–	4.0	3.5
8Au-CL(UGC)	158.1	49.1, 36.6[i]	4.5	4.5
CL(CP)[a]	72.2	–	7.4	7.0
CL(CP)[b]	48.0	–	11.6	9.9
CL(UGC)[a]	161.6	–	5.1	4.8
CL(UGC)[b]	93	–	7.1	6.9
C4L(UGC)[b]	69.1	–	8.1	8.5
CL(UGC)[d]	41.9	–	11	10.8

[a] CL calcined at 400 °C in air.
[b] CL or C4L calcined at 650 °C in air.
[c] Catalyst calcined at 650 °C in air.
[d] Calcined at 800 °C in air.
[e] Determined by XRD, using the Scherrer equation.
[f] Used in 7% CO–38% H_2O–11% CO_2–40% H_2–He for 120 h.
[g] Used in 2% CO–10% H_2O–He for 70 h.
[h] No copper compounds detected by XRD.
[i] Au⟨200⟩.

3.2. H_2-TPR

Temperature-programmed reduction by H_2 has been used extensively in the literature to characterize the oxygen reducibility of doped CeO_2. Yao *et al.* [8] reported that the reduction peaks of the surface capping oxygen and the bulk oxygen of CeO_2 are centered at 500 and 800 °C, respectively. It is well known that the TPR profile of ceria as well as that of other solid materials is determined by four main factors, namely, the thermodynamics and kinetics of reduction, the textural changes of the material and oxygen diffusion in the lattice structure [36]. For low specific surface area ceria, Johnson and Mooi [37] developed a simple model, which stated that hydrogen consumption is only related to the specific surface area of ceria. However, this model is restricted to a narrow surface area range. Chiang *et al.* [38] reported that high surface area nanocrystalline ceria has a lower reduction enthalpy than that measured for the bulk material. Trovarelli and his coworkers [9,39] have reported that reduction of ceria strongly depends on the ceria crystallite size. The reduction behavior of ceria can be dramatically changed by the addition of a small amount of Pt metals [8,9,40] or base metals [1,4,31,32]. The first peak corresponding to the reduction of surface oxygen can be shifted to much lower temperatures, although the reduction of bulk oxygen still remains near 800 °C. Jen *et al.* [40] showed that the 500 °C-peak was shifted to below 100 °C by the addition of PdO. The hydrogen consumption is partially due to the reduction of metal oxide and partially due to the reduction of ceria [9,40,41]. In turn, ceria enhances the reducibility of supported metal oxides [1,4,32]. While bulk CuO is reduced at 200–300 °C, the reduction peaks of ceria-supported copper oxide are all below 180 °C [1,31,42].

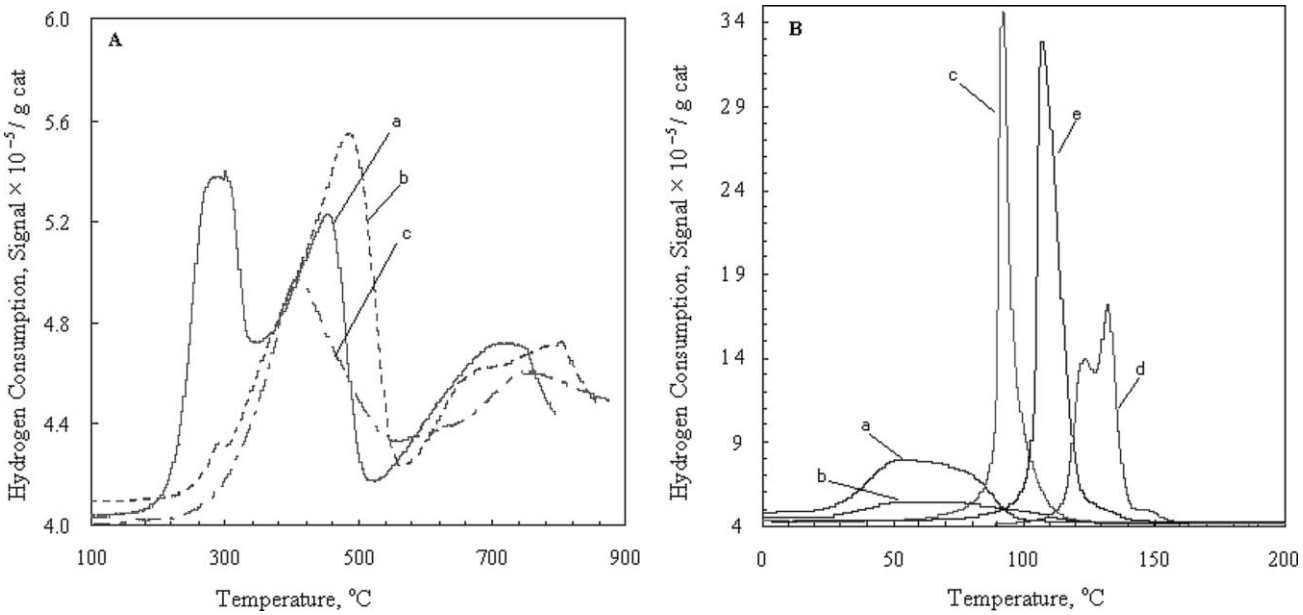

Figure 4. H_2-TPR profiles of ceria-based samples. (A) (a) CL(CP) calcined at 400 °C; (b) CL(UGC) calcined at 400 °C; (c) CL(UGC) calcined at 650 °C. (B) (a) 4.7Au-CL(DP)[a]; (b) 4.5Au-CL(DP)[b]; (c) 3.8Au-CL(CP); (d) 5Cu-CL(UGC)[c]; (e) 8Au-CL(UGC). 20% H_2/N_2, 50 cm^3/min (NTP), 5 °C/min. See table 1 for sample identification and preparation conditions.

H_2-TPR has also been used to identify potentially higher oxidation states of gold on supports. Kang and Wan [43] reported that Au/Y-zeolite possessed two reduction peaks (at 125 and 525 °C) and one shoulder peak (at 190 °C). They attributed the first peak to oxygen adsorbed on surface metallic gold and the second to reduction of Au(III) located in sodalite cages. For supported Au/Al_2O_3 samples made by deposition–precipitation [44], three reduction peaks (at $T_r = -90$, 30, and 720 °C) were found by H_2-TPR and, respectively, assigned to reductions of Au^sO, Au^sCl, and Au^i ions. Neri *et al.* [45] reported two separated peaks (125 and 175 °C) for "as-prepared" Au/Fe_2O_3 without calcination. However, after oxidation at 300 °C, only one peak (165 °C) was observed. It was surmised that the first peak belongs to the reduction of Au oxide or hydroxide, which decomposes in calcination above 300 °C [13,14].

In this work, TPR was carried out with several CL(UGC or CP) and Au-CL(DP or CP) catalysts. A copper–ceria sample, 5Cu-CL(UGC), was also included in this study for comparison. Figure 4 shows the hydrogen consumption by some of these materials. The reduction peak temperature and corresponding hydrogen consumption are listed in table 2. The key finding from this analysis is that the surface oxygen of ceria is substantially weakened by the presence of gold nanoparticles, its reduction temperature shifting by several hundred degrees to 100 °C or lower. Exactly how much weaker this oxygen becomes depends strongly on the preparation method, metal loading, and calcination temperature.

The onset of oxygen reduction changes with the type of support, as shown in figure 4(A). CL(UGC) calcined at 400 °C, began to reduce at 350 °C with a peak at 487 °C, which is assigned to the surface capping oxygen of CeO_2 [8]. CL(UGC) calcined at 650 °C has the same reduction profile,

Table 2
Reducibility of ceria-based materials. (Measured by H_2-TPR; 20% H_2/N_2 gas mixture (50 cm^3/min (NTP)), 5 °C/min. All catalysts are as prepared and calcined at 400 °C, unless otherwise noted; CL: Ce(10% La)O_x.)

Sample	H_2 consumption (μmol/g-cat)			x in CeO_x		
	Peak 1 (T, °C)	Peak 2 (T, °C)	Peak 3 (T, °C)	Peak 1	Peak 2	Peak 3
0.9Au-CL(DP)[b]	165 (69)	329 (109)		1.97	1.90	
4.7Au-CL(DP)[b]	213 (51)	198 (68)		1.96	1.92	
4.7Au-CL(DP)[b,c]	132 (84)	289 (107)		1.97	1.91	
8.3Au-CL(DP)[b]	98 (40)	306 (59)		1.98	1.91	
4.5Au-CL(DP)[a]	560 (55)	192 (79)		1.89	1.85	
3.8Au-CL(CP)	803 (96)			1.84		
0.9Au-CL(CP)	672 (160)			1.87		
8Au-CL(UGC)	903 (110)			1.81		
5Cu-CL(UGC)[c,d]	275 (126)	282 (132)	175 (145)	1.95	1.89	1.86
5Cu-CL(UGC)[d]	633 (150)	396 (224)	39 (246)	1.88	1.80	1.79
CL(CP)[a]		431 (310)	455 (497)		1.92	1.83
CL(UGC)[a]			706 (487)			1.87
CL(UGC)[b]			425 (437)			1.92
CeO_2(CP)[a]			782 (405)	1.87		

[a] CL calcined at 400 °C in air.
[b] CL calcined at 650 °C in air.
[c] Sample calcined at 650 °C in air.
[d] x is calculated after subtracting the oxygen from CuO reduction to Cu.

but a much smaller peak area, attributed to the lower surface area of this sample. CL(CP) calcined at 400 °C shows two reduction peaks for surface oxygen, one at 310 °C and a second at 497 °C. The latter is at the same position as for CL made by UGC. The first peak maybe due to the interaction of lanthana with ceria as reported by Groppi *et al.* [46] for the ternary $CeO_x/LaO_x/Al_2O_3$ material. This is also supported by the absence of a first reduction peak at 310 °C in the TPR profile of undoped ceria (CP), table 2. The total hydrogen consumption is larger for the CP sample than for CL made

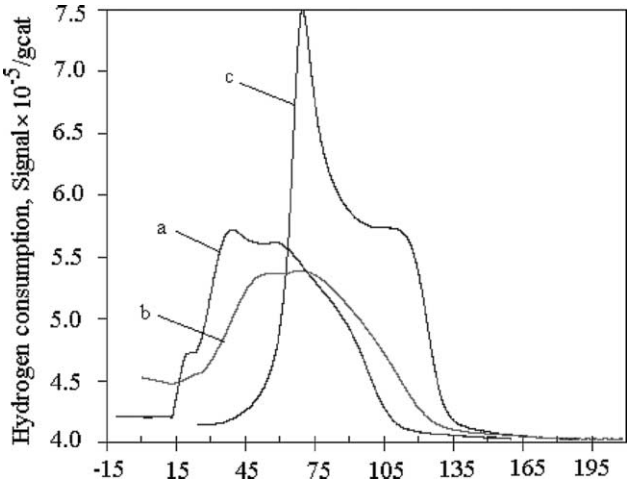

Figure 5. H_2-TPR profiles of Au-ceria catalysts prepared by deposition–precipitation: (a) 8.3Au-CL(DP)[b]; (b) 4.5Au-CL(DP)[b]; (c) 0.9Au-CL(DP)[b]; 20% H_2/N_2, 50 cm^3/min (NTP), 5 °C/min. See table 1 for sample identification and preparation conditions.

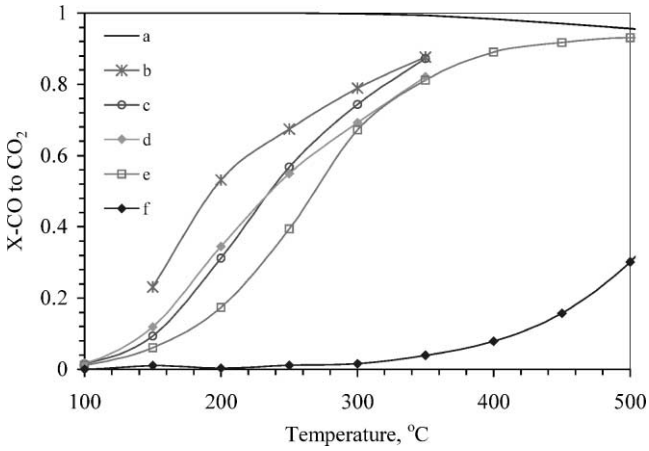

Figure 6. Water–gas-shift reactivity of several ceria-based catalysts. 0.09 g s/cm^3 (NTP), 2% CO–10.7% H_2O–He; (a) equilibrium line at this condition, (b) 4.5Au-CL(DP)[a], (c) 3.8Au-CL(CP), (d) 4.7Au-CL(DP)[b], (e) 5Cu-CL(UGC)[c], (f) CL(UGC)[b]. See table 1 for sample identification and preparation conditions.

by UGC, which might due to the different structures formed during preparation by the CP and UGC techniques.

Regardless of the type of ceria or addition of metal, a peak at 700 °C corresponding to reduction of bulk oxygen of CeO_2, remains unchanged for all samples. This is similar to the case of Pt metals supported on ceria [9,40] or on ceria–zirconia oxide solid solutions [40]. Other transition metals and metal oxides on ceria have a similar effect [1,4–7,31,42]. In previous work, we found a clear reducibility enhancement of ceria by copper in the Cu/ceria system [1,4,31,42]. Presently, from the TPR data of figure 4(B) and table 2, it is observed that the effect of gold on ceria reducibility is stronger than that of CuO. The reducibility is expressed by the value of x in CeO_x in table 2. This is calculated from the hydrogen consumption. For the Cu-containing samples, a complete reduction of CuO is assumed before calculating the x value. The peaks corresponding to the reduction of surface capping oxygen of ceria in the Au–ceria samples became much sharper and shifted to lower temperatures. The DP sample started to reduce around room temperature with a peak at 59 °C. Reduction on the CP sample began at 70 °C with a peak at 96 °C. The peak areas were similar to the peak area of the corresponding Au-free ceria sample, as seen in table 2. This suggests that most gold is in metallic state.

Figure 5 clearly shows that gold facilitates the reduction of ceria surface oxygen species. Increasing gold loading in the DP samples, weakens this oxygen further. For instance, the 8.3Au-CL(DP) sample has two reduction peaks with peak temperature at 40 and 59 °C, while 0.9Au-CL(DP) has two reduction peaks with peak temperatures at 69 and 109 °C. All these samples have similar total peak areas, as shown in figure 5 and table 2. Thus, the addition of gold does not increase the hydrogen consumption. However, it drastically increases the oxygen reducibility. Since the TPR technique is not as sensitive to surface oxygen titration, the effect of gold loading on the surface oxygen reducibility can be better followed by a pulse titration technique [40]. Accordingly, addition of gold was found to increase dramatically the oxygen storage capacity of ceria, especially at temperatures below 350 °C [30].

3.3. Activity studies

Figure 6 shows CO conversions over ceria, Cu-CL, and Au-CL samples at contact time 0.09 g s/ml, and a feed gas of 2% CO–10% H_2O–He. Kinetics data at two temperatures, 100 and 175 °C, are shown in table 3. No activation was necessary for these catalysts. As shown by the shift of the reaction light-off temperature to lower values, both copper and gold-containing cerium oxide are superior WGS catalysts compared to CL. Notably, higher than 80% CO conversion was measured at 350 °C over the metal oxide-containing ceria, while the corresponding CO conversion over CL was less than 5% at this temperature.

Figure 7 shows the CO conversion profiles with temperature over samples containing different gold loading (prepared by DP) and the 8Au-CL(UGC) sample. For the DP samples, this figure and table 1 show that with a similar gold particle size, the conversion increases with gold loading. The ceria particle size in the DP samples is also the same, 7 nm. It is interesting to explain the improved conversion over the 8Au-CL(UGC) sample, which has the same Au loading as one of the DP samples. The conversion over this sample is higher, despite the much larger size (42 nm) of its gold particles. What is different in this sample is the small particle size (4.5 nm) of ceria. Thus, a key parameter for WGS activity is the ceria particle size. However, in the absence of gold, the same size ceria material, figure 7, is not active at low temperatures.

Bollinger and Vannice [47] reported that a TiO_2-covered Au powder, which contained large Au (10 μm) and small TiO_2 crystallites, showed high activity for CO oxidation. Au/TiO_2 made by impregnation with ∼25 nm gold parti-

Table 3
WGS reaction rates over various catalysts. (All catalysts are as prepared and calcined at 400 °C, unless otherwise noted; CL: Ce(10% La)O_x.)

Sample	Reaction conditions	Rate × 10^7 (mol/g-cat s)	Rate × 10^9 (mol/(m-cat)^2 s)	Ref.
$Cu/ZnO/Al_2O_3$[a]	100 °C, 1% CO–2% H_2O	1.2	–	[17]
5% Au/TiO_2[b]	100 °C, 1% CO–2% H_2O	1.4	2.8	[17]
3.8Au-CL(CP)	100 °C, 1% CO–2% H_2O	4	5.6	This work
4.5Au-CL(DP)[c]	100 °C, 1% CO–2% H_2O	2.9	1.9	This work
Rh/CeO_2[d]	175 °C, 2.5% CO–2% H_2O	0.2	2.3	[2]
5Cu-CL(UGC)[e]	175 °C, 1% CO–2% H_2O	15	17	[1]
3.8Au-CL(CP)	175 °C, 1% CO–2% H_2O	22	31	This work
4.5Au-CL(DP)[c]	175 °C, 1% CO–2% H_2O	34	22	This work
4.7Au-CL(DP)[f]	175 °C, 1% CO–2% H_2O	14	17	This work

[a] [17] commercial catalyst provided by Catalysts and Chemicals Inc., Far East (Japan).
[b] [17] Au/TiO_2, prepared by deposition–precipitation, calcined at 400 °C.
[c] CL calcined at 400 °C in air.
[d] [2] prepared by vapor deposition, calcined at 297 °C.
[e] Catalyst calcined at 650 °C in air.
[f] CL calcined at 650 °C in air.

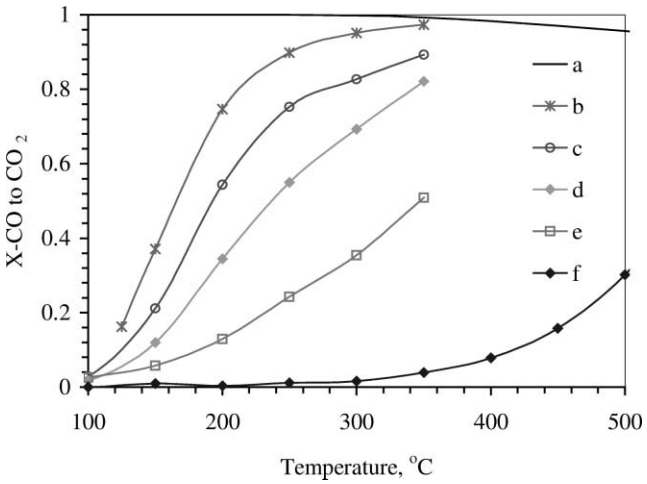

Figure 7. Effect of gold loading and ceria particle size on WGS conversion; 0.09 g s/cm^3 (NTP), 2% CO–10.7% H_2O–He: (a) equilibrium line, (b) 8Au-CL(UGC), (c) 8.3Au-CL(DP)[b], (d) 4.7Au-CL(DP)[b], (e) 0.9Au-CL(DP)[b], (f) CL(UGC)[b]. See table 1 for sample identification and preparation conditions.

cle size, produced comparable activity as Au/TiO_2 made by coprecipitation [22,47]. They suggested that the interfacial effect to get more active sites created by metal–support interaction is more important than the electronic effect by decreasing gold particle size. Schubert *et al.* [20] hypothesized that the TOF of CO oxidation is independent of the size of gold particle supported on reducible oxides, since the reactive oxygen is provided by the support. On the other hand, dissociative oxygen adsorption on Au particles supported on inert oxide is controlled by the gold particle size.

Compared with other supported gold catalysts for which WGS reaction rates have been measured, as shown in table 3, Au–ceria is comparable to Cu–ceria [11] and better than Au/TiO_2 [17]. The WGS rate of Au–ceria prepared by CP is twice as high as the rate over Au/TiO_2. While both of these supports are reducible, the storage capacity of ceria is much higher than that of TiO_2.

During a 120 h-long stability test, the 4.7Au-CL(DP) catalyst activity remained the same, in a reformate-type gas mixture containing 7% CO–38% H_2O–11% CO_2–40% H_2–bal. He at 300 °C. No significant changes were observed in the conversion of CO in this test period. Catalyst characterization after this test, found that the ceria particle size increased only slightly, while the gold particle size grew to 6.7 nm, as shown in figure 3 and table 1.

On the basis of all the above findings, we conclude that the Au particle size is not the most important factor for the WGS reaction, because the oxygen for the WGS reaction is supplied by ceria. The particle size of the latter is very important, however, for oxygen transfer [38]. The presence of gold is important because CO adsorption takes place on gold. It is known that on hydroxylated ceria, CO adsorption is completely hindered [48]. Thus, a cooperative redox mechanism for the WGS reaction on Au–ceria is plausible, similar to what we have found for Cu–ceria [11] and similar to what has been reported for the Pt metals/ceria [2]. Detailed kinetic and mechanistic studies to test this are currently underway.

4. Conclusions

The structure, reducibility, and WGS reactivity of gold–ceria materials made by deposition–precipitation, coprecipitation or gelation methods were examined in this work. Nanosized ceria and gold particles co-exist in the Au–ceria composites. The addition of gold significantly increases the reducibility of the ceria surface oxygen. The amount of surface oxygen available for reduction is controlled by the crystal size of ceria.

Au–ceria is a very active and stable catalyst for the water–gas shift reaction. Its catalytic activity correlates well with its reducibility.

Acknowledgement

The financial support of this work by the NSF/EPA, Grant #CTS-9985305, is gratefully acknowledged. AW also acknowledges the support of the US EPA, STAR fellowship #U-915348.

References

[1] Y. Li, Q. Fu and M. Flytzani-Stephanopoulos, Appl. Catal. B 27 (2000) 179.
[2] T. Bunluesin and R.J. Gorte, Appl. Catal. B 15 (1998) 107.
[3] T. Bunluesin, H. Cordatos and R.J. Gorte, J. Catal. 157 (1995) 222.
[4] W. Liu, Sc.D. dissertation, Department of Chemical Engineering, MIT (1995).
[5] W. Liu and M. Flytzani-Stephanopoulos, J. Catal. 153 (1995) 304.
[6] W. Liu and M. Flytzani-Stephanopoulos, J. Catal. 153 (1995) 317.
[7] A. Weber, M.S. thesis, Department of Chemical Engineering, Tufts University (1999).
[8] H.C. Yao and Y.F. Yu Yao, J. Catal. 86 (1984) 254.
[9] A. Trovarelli, Catal. Rev. Sci. Eng. 38 (1996) 439.
[10] Y. Li, M.S. thesis, Department of Chemical Engineering, Tufts University (1998).
[11] Q. Fu, Y. Li, A. Weber and M. Flytzani-Stephanopoulos, in: *Annual AIChE Meeting*, paper #41f, Los Angeles, CA, 12–17 November 2000.
[12] S. Gardner, G. Hoflund, D. Schryer, J. Schryer, B. Upchurch and E. Kielin, Langmuir 7 (1991) 2135.
[13] M. Haruta, N. Yamada, T. Kobayashi and S. Iijima, J. Catal. 115 (1989) 301.
[14] M. Haruta, S. Tsubota, T. Kobayashi, J. Kageyama, M.J. Genet and B. Delmon, J. Catal. 144 (1993) 175.
[15] M. Haruta, Catal. Today 36 (1997) 153.
[16] D. Andreeva, V. Idakiev, T. Tabakova and A. Andreev, J. Catal. 158 (1996) 354.
[17] H. Sakurai, A. Ueda, T. Kobayashi and M. Haruta, Chem. Commun. (1997) 271.
[18] F. Boccuzzi, A. Chiorina, M. Manzoli, D. Andreeva and T. Tabakova, J. Catal. 188 (1999) 176.
[19] T. Tabakova, V. Idakiev, D. Andreeva and I. Mitov, Appl. Catal. A 202 (2000) 91.
[20] M.M. Schubert, S. Hackenberg, A.C. van Veen, M. Muhler, V. Plzak and R.J. Behm, J. Catal. 197 (2001) 113.
[21] A.I. Kozlov, A.P. Kozlova, H. Liu and Y. Iwasawa, Appl. Catal. A 182 (1999) 9.
[22] S.D. Lin, M. Bollinger and M.A. Vannice, Catal. Lett. 17 (1993) 245.
[23] S. Tsubota, D.A.H. Cunningham, Y. Bando and M. Haruta, *Preparation of Catalysts VI*, eds. G. Poncelet et al. (Elsevier, Amsterdam, 1995) p. 275.
[24] T. Kobayashi, M. Haruta, S. Tsubota and H. Sano, Sens. Actuators B1 (1990) 222.
[25] M. Okumura, K. Tanaka, A. Ueda and M. Haruta, Solid State Ionics 95 (1997) 143.
[26] A.P. Kozlova, A.I. Kozlov, S. Sugiyama, Y. Matsui, K. Asakura and Y. Iwasawa, J. Catal. 181 (1999) 37.
[27] J.D. Grunwaldt, C. Kiener, C. Wogerbauer and A. Baiker, J. Catal. 181 (1999) 223.
[28] Y. Amenomiya, A. Emesh, K. Oliver and G. Pleizer, in: *Proc. 9th Int. Congress on Catalysis*, Chemical Institute of Canada, Ottawa, Canada, eds. M. Philips and M. Ternan (1988) p. 634.
[29] J.W. Niemantsverdriet, *Spectroscopy in Catalysis* (VCH, New York, NY, 1995).
[30] Q. Fu, Ph.D. dissertation, Tufts University, in progress.
[31] L. Kundakovic and M. Flytzani-Stephanopoulos, J. Catal. 179 (1998) 203.
[32] Lj. Kundakovic, Ph.D. dissertation, Department of Chemical Engineering, Tufts University (1998).
[33] C. Sze, E. Gulari and B.G. Demczyk, Mater. Lett. 36 (1998) 11.
[34] Y.M. Kang and B.Z. Wan, Appl. Catal. A 128 (1995) 53.
[35] M. Haruta, T. Kobayashi, S. Iijima and F. Delannay, in: *Proc. 9th Int. Congress on Catalysis*, Calgary, Vol. 2, eds. M.J. Phillips and M. Ternan (The Chemical Institute of Canada, Ottawa, 1988) p. 1206.
[36] A. James and B. McNicol, in: *Temperature-Programmed Reduction for Solid Materials Characterization* (Dekker, NY, 1986).
[37] M.F.L. Johnson and J. Mooi, J. Catal. 103 (1987) 502.
[38] Y.M. Chiang, E.B. Lavik, I. Kosacki, H.L. Tuller and J.Y. Ying, J. Elelctroceram. 1 (1997) 7.
[39] A. Trovarelli, C. deLeitenburg, G. Polcetti and J. Llorca, J. Catal. 151 (1995) 111.
[40] H.W. Jen, G.W. Graham, W. Chun, R.W. McCabe, J.P. Cuif, S.E. Deutsch and O. Touret, Catal. Today 50 (1999) 309.
[41] J. Cunningham, D. Cullinane, J. Sanz, J.M. Rojo, X.A. Soria and J.L.G. Fierro, J. Chem. Soc. Faraday Trans. 88 (1992) 3233.
[42] W. Liu and M. Flytzani-Stephanopoulos, Chem. Eng. J. 64 (1996) 283.
[43] Y. Kang and B. Wan, Catal. Today 35 (1997) 379.
[44] C.K. Chang, Y. Chen and C. Yeh, Appl. Catal. A 174 (1998) 13.
[45] G. Neri, A.M. Visco, S. Galvagno, A. Donato and M. Panzalorto, Therm. Acta 329 (1999) 39.
[46] G. Groppi, C. Cristiani, L. Lietti, C. Ramella, M. Valentini and P. Forzatti, Catal. Today 50 (1999) 399.
[47] M.A. Bollinger and M.A. Vannice, Appl. Catal. B 8 (1996) 417.
[48] C. Li, K. Domen, K.I. Maruya and T. Onishi, J. Catal. 123 (1990) 436.